Microporous and Mesoporous Materials 243 (2017) 85–90

Contents lists available at ScienceDirect

Microporous and Mesoporous Materials

journal homepage: www.elsevier.com/locate/micromeso

Monitoring instability of linear amine impregnated UiO-66 by in-situ temperature resolved powder X-ray diffraction

Youngdong Song [a], Damien Thirion [a], Saravanan Subramanian [a], Myoung Soo Lah [b], Cafer T. Yavuz [a, c, *]

[a] Graduate School of EEWS, Korea Advanced Institute of Science and Technology (KAIST), Daejeon 34141, Republic of Korea
[b] Department of Chemistry, Ulsan National Institute of Science and Technology, UNIST-gil 50, Ulsan 44919, Republic of Korea
[c] Department of Chemistry, Korea Advanced Institute of Science and Technology (KAIST), Daejeon 34141, Republic of Korea

ARTICLE INFO

Article history:
Received 5 December 2016
Received in revised form
3 February 2017
Accepted 6 February 2017
Available online 9 February 2017

Keywords:
Carbon capture
Microporous materials
Amine impregnation

ABSTRACT

Carbon dioxide capture requires stable porous solids like zirconium based metal-organic frameworks (MOFs) in order to make sequestration efforts feasible. Because of the weak binding at low CO_2 partial pressures, oligomeric amines are commonly loaded on porous supports to maximize CO_2 capture while attempting to keep porosity for enhanced diffusion. Here we show the first temperature resolved stability study of linear-amine impregnated UiO-66 by in-situ monitoring of the PXRD pattern. Our findings show that the crystal structure shows a contraction at temperatures as low as 80 °C and deforms considerably above 120 °C, leading to significant doubts about their applicability in CO_2 capture from lean feeds. We confirm that all MOFs need to be thoroughly analyzed at least by means of PXRD at the process relevant temperatures, and reinforced before any plausible plans of application in CO_2 capture.

1. Introduction

Steadily increasing carbon dioxide (CO_2) concentration in the atmosphere has been causing severe global issues such as global warming and climate change [1,2]. The tendency of surging CO_2 concentration will not be altered without global and urgent actions. In order to reduce the major anthropogenic greenhouse gas emissions, scientific research has focused on capturing CO_2 in flue gas mixture emitted from power plants, which accounts for the most emissions of CO_2 [3].

To date, many technologies were proposed for efficient CO_2 capture [4,5]. Currently, amine scrubbing is the most prevailing method in which CO_2 is removed by about 30% of monoethanolamine (MEA) solutions in water [6]. In MEA solutions, CO_2 is chemically captured by amine molecules in the form of carbamate/carbamic acid, and desorbed by thermal treatment of saturated solution. However, this process requires massive heat to regenerate the amine solution, and the corrosive nature of amine solutions is detrimental to the amine scrubber [7,8].

In order to overcome such economic and environmental problems, porous solids have gained increased attention as alternative sorbents [9–12]. Unlike amine solutions, porous solids have been thought to be more promising because they do not require the presence of water, which does not participate in the capture, but requires exorbitant heat for regeneration due to its high heat capacity. Also, these porous solids are not corrosive, so that scrubber life expectancy will be extended [4].

There have been extensive studies to utilize porous solids for CO_2 capture [13,14]. One of the most compelling methods is amine loading in porous solids [15]. In general, amine molecules or polyethyleneimine (PEI) polymers are loaded chemically (grafting) or physically (impregnation) into porous solids such as carbons, mesoporous silica, porous polymers, and MOFs [16–19]. Physical amine impregnation is generally regarded as more viable method because higher amine concentration could be achieved in porous solids and thus provides enhanced CO_2 uptake capacity [20,21].

In the last decade, metal-organic frameworks (MOFs) have been studied extensively as a promising candidate for CO_2 capture [16,22–33]. MOFs consist of inorganic metal clusters, so-called secondary building units (SBUs), repetitively coordinated by organic linkers to give highly crystalline structures with

* Corresponding author. Graduate School of EEWS and Dept. of Chemistry, Korea Advanced Institute of Science and Technology (KAIST), 373-1 Guseong-dong, Yuseong-gu, Daejeon, 305-701, Republic of Korea.
E-mail address: yavuz@kaist.ac.kr (C.T. Yavuz).
URL: http://yavuz.kaist.ac.kr, http://www.twitter.com/caferyavuz

http://dx.doi.org/10.1016/j.micromeso.2017.02.021
1387-1811/

outstanding surface area and porosity. The final crystal structures can be designed by choosing different inorganic nodes and organic linkers, which enables a myriad of tailored structures [34,35]. In addition, organic linkers possessing functional groups can be further tuned by post synthetic modification without affecting crystal structure of original MOFs [36–38]. Coordinatively unsaturated open metal sites of metal centers also show interesting behaviors with guest molecules, so that comprehensive studies have been focused on applications regarding these significant properties [39–44].

In post-combustion CO_2 capture by MOFs, water stability of MOFs is a decisive factor because flue gas contains 5–7% humidity [7]. As perfect removal of omnipresent water is restrictive, moisture sensitivity of MOFs has been a major limitation in industrial applications [45]. In general, it has been known that basicity of organic linkers, the extent of coordination between inorganic clusters and organic linkers, and hydrophobicity of functional groups in organic linkers affect moisture stability of MOFs by displacement of organic linkers from inorganic clusters [45]. In order to overcome moisture sensitivity, scientists have attempted strategies such as increasing extent of coordination between SBU and organic linkers, or assigning hydrophobicity in the structure [46,47].

Of all MOFs studied for CO_2 capture, one leading example is UiO-66 (UiO refers to University of Oslo) [48–50]. In UiO-66, oxo-hydroxo-zirconium clusters are linked by 1,4-benzenedicarboxylate to form a porous network of a 12-c **fcu** topology [51]. Unlike other MOFs, UiO-66 is well-known for its unprecedented stability because of the highest coordination found in MOFs [32]. Strong oxophilicity of zirconium also makes coordination between inorganic clusters and organic linker outstanding [52].

Amine loaded UiO-66 have been studied extensively for CO_2 capture. Li et al. synthesized MEA grafted UiO-66 for CO_2 capture from flue gas [53]. They added dilute MEA/toluene solution after dehydration of UiO-66 at 300 °C in which MEA molecules tethered on the dehydrated zirconium oxide clusters. MEA modified UiO-66, $[Zr_6O_4(OH)_2(MEA)_2(bdc)_6]$, exhibited 2.5 times higher CO_2 uptake than pristine UiO-66 does. More importantly, the adsorption enthalpy of MEA modified UiO-66 was −66 kJ/mol, which was twice higher than UiO-66. Xian et al. reported polyethyleneimine (PEI) impregnated UiO-66 to show enhanced CO_2 adsorption dynamics [54]. In their study, 30% PEI loading in UiO-66 was tested for separation of CH_4/CO_2 mixture by breakthrough experiment. CO_2 working capacity and CO_2/CH_4 selectivity were enhanced by 5.7 times and 5.3 times at 308 K, respectively. The value was increased further at higher temperature (338 K), which is attributed to facile diffusion of CO_2 molecules into pore structures.

Despite all the interest, a close in-situ monitoring while raising temperature of amine impregnated UiO-66 has not been performed. This is particularly important because the regeneration of CO_2 adsorbents is mainly based on temperature swings, in that CO_2 is captured at low temperature and desorbed at high temperature. Sorbents are expected to be stable in these cycles without loss of performance or deterioration of structure. In temperature swing adsorption (TSA) process, adsorption and desorption cycle should occur between 40 °C and 150 °C [55]. As the temperature of flue gas released from power plants is 40–50 °C, CO_2 should be adsorbed in this temperature range without further energy demand in cooling, and recommended desorption temperature is 100–200 °C.

In this study, we investigate changes in PXRD patterns of linear amine impregnated UiO-66 with temperature cycle to 200 °C primarily by in-situ temperature resolved PXRD. We show that one of linear amine, namely pentaethylenehexamine (PENTAEN), impregnated UiO-66 shows severe peak broadening with peak shift to higher 2 theta region and conspicuous decrease in intensity. The attenuated and broadened peak pattern is not recoverable even when temperature was decreased again. However, pristine UiO-66 shows flexible and slight 2θ shift, but intensity was retained in the same condition. In this regard, although amine impregnated UiO-66 seems stable in ambient temperature, it is susceptible at high temperature required for regeneration of sorbents. As the process of high temperature in-situ PXRD monitoring is similar to regeneration of solid adsorbents, CO_2 uptake and BET surface area were also measured in different PENTAEN loading. Furthermore, several linear amines generally used for improvement in CO_2 capacity were impregnated in UiO-66 after dehydration in order to show chemical stability of dehydrated UiO-66 with linear amines frequently used for CO_2 capture (see Fig. 1).

2. Experimental

2.1. Materials

$ZrCl_4$ and terephthalic acid were purchased from Sigma Aldrich, USA. Hydrochloric acid (HCl, 35–37%), ethylenediamine (EN), and diethylenetriamine (DIEN) were purchased from SAMCHUN, South Korea. Triethylenetetramine (TRIEN), tetraethylenepentamine (TETRAEN), and pentaethylenehexamine (PENTAEN) were purchased from TCI, Japan. *N*,*N*′-dimethylformamide (DMF) was purified by solvent distillation equipment.

2.2. Synthesis

UiO-66 was synthesized according to the reported literature with slight modification [56]. $ZrCl_4$ (417.5 mg) was added to dry DMF (15 mL) in a glass vial (100 mL). Concentrated HCl (3.34 mL) was added to the dispersion and sonicated for 20 min to get a transparent solution. Terephthalic acid (410.9 mg) and dry DMF (35 mL) were added to the solution and sonicated another 20 min. The mixture turned transparent after sonication. After the vial was sealed with Teflon tape and a cap, the transparent solution was heated at 120 °C for 24 h. White dispersion was observed during the process, and the product was collected by centrifugation (8000 rpm, 1000s, 25 °C) and washed with DMF three times and soaked in methanol. Methanol was exchanged every 24 h for 3 days. The resulting solid was dried at 100 °C for 6 h under vacuum.

UiO-66-PENTAEN-X for surface area and CO_2 adsorption analysis. As-synthesized UiO-66 was dehydrated at 250 °C for 6 h under vacuum. Dehydrated UiO-66 (200 mg) was added to each concentration of PENTAEN/methanol solution, and stirred for 24 h. UiO-66-PENTAEN composite was collected by centrifugation and dried at 150 °C for 6 h under vacuum. X refers to the amount of PENTAEN in 20 mL methanol solution. X = 100 (200 mg of PENTAEN), 200 (400 mg of PENTAEN), 300 (600 mg PENTAEN), 400 (800 mg PENTAEN), 500 (1000 mg PENTAEN).

UiO-66-linear amines for linear amine variation test. Linear amines (EN, DIEN, TRIEN, TETRAEN, and PENTAEN) were stored on activated molecular sieve (4A, 8–12mesh) for 24 h in order to remove water molecules in hygroscopic amines. Each amine (5 mL) was added to UiO-66 (200 mg) previously activated at 250 °C under vacuum for 6 h, and the mixture stirred for 24 h. The resulting solid was recovered by centrifugation, and dried in a desiccator filled with silica gel at room temperature.

UiO-66-PENTAEN for in-situ temperature resolved PXRD. As-synthesized UiO-66 (600 mg) was added to dry PENTAEN (5 mL). The mixture was stirred for 24 h. The mixture was washed with methanol twice and dried in a desiccator filled with silica gel.

2.3. Characterization

Thermogravimetric analysis (TGA) were performed on DTG-60A, Shimadzu. The samples were heated under nitrogen flow (50 mL/min) with a ramp of 10 °C/min up to 800 °C. Nitrogen content was obtained with Flash 2000 series, Thermo Scientific. Nitrogen sorption isotherms and CO_2 uptake were performed on 3flex, Micromeritics. The samples were degassed at 150 °C under vacuum for 6 h before measurement. Small-angle X-ray scattering (SAXS) was performed on a D/MAX-2500, by Rigaku. Powder X-ray diffraction pattern (PXRD) patterns were collected on Smartlab, Rigaku with Cu Kα radiation (λ = 1.5418 Å). PXRD Patterns were collected in 5–50° 2θ range with a scan speed of 2 °C/min and step size was 0.01°. In-situ temperature resolved PXRD patterns were performed on D/MAX-2500, Rigaku. In-situ temperature resolved PXRD patterns were collected under vacuum (10^{-3} torr) at programmed temperature with 5 min stabilization time. Temperature was increased with a ramp of 2 °C/min.

3. Results and discussion

Synthesis of UiO-66 is straightforward and well established. Typically, $ZrCl_4$, terephthalic acid, and HCl were heated in DMF to afford white crystal powder [56]. DMF is generally exchanged to other solvents having lower boiling point such as methanol or ethanol because the resulting powder still contains significant amounts of trapped DMF, which is difficult to remove (without destroying the crystal) by simple thermal treatment. In this study, methanol was used due to its low boiling point.

As-synthesized UiO-66 was characterized by SAXS up to a 2 theta value of 10° in order to confirm the thermal stability of bare UiO-66 without activation. According to Shearer et al., thermal stability of UiO-66 considerably depends on the synthetic procedures [57]. To be specific, possibly unstable UiO-66 shows two broad symmetry forbidden reflections at 2 theta value of 4.2° and 6.0° in PXRD pattern. Also, this forbidden reflection is marked after methanol exchange step. However, two forbidden reflections were not observed in the bare UiO-66 even after three times of methanol exchange, meaning that synthesized UiO-66 was stable and defect-free (Fig. S1). Upon heating UiO-66, it is known that open metal sites form by the dehydration of SBUs [$Zr_6O_4(OH)_4$] into [Zr_6O_6] by losing two water molecules [48]. When we heated as-synthesized UiO-66 at 250 °C under vacuum for 6 h, the PXRD pattern was similar to the as-synthesized UiO-66 (UiO-66-250V) (Fig. S2), which means the crystal structure is retained at high temperature under vacuum as expected. Addition of methanol to dehydrated UiO-66 (UiO-66-250V-MeOH) also did not affect the PXRD pattern. However, addition of PENTAEN/methanol solution to dehydrated UiO-66 (UiO-66-PENTAEN-500-as synthesized) results in the significant broadening of the PXRD. This is attributed to the presence of PENTAEN because PXRD pattern of UiO-66 was not affected by pure methanol addition. Li et al. also attempted to modify pristine UiO-66 by soaking UiO-66 in pure MEA, which resulted in an amorphous material [53]. They suspected that the strong coordination ability of MEA decomposed the crystal structure of UiO-66. The heating of UiO-66-PENTAEN-500 at 150 °C under vacuum (UiO-66-PENTAEN-500-150V) even further accelerates the collapse of the PXRD pattern. Since this undesired observation is detrimental to the potential use for CO_2 capture, we decided to study further using in-situ temperature resolved PXRD analysis.

The PXRD patterns of as-synthesized UiO-66 look intact (Fig. 2). However, when we focus on the low angle diffraction region (7-9°), the two peaks shift to higher angles when temperature raised, but return back to the original position when temperature was decreased to room temperature. This phenomenon occurs in all patterns obtained (5-50°). This negative thermal expansion has been commonly observed in MOFs, but only Hf based UiO-66 has been reported in UiO-66 structures (ref) [58,59]. This shows that Zr based UiO-66 also undergoes negative thermal expansion.

In order to verify whether the structural integrity is preserved, we studied PXRD patterns of PENTAEN impregnated UiO-66 by in-situ temperature resolved PXRD under vacuum. In a typical run, temperature was increased up to 200 °C with a ramp of 2 °C/min under vacuum (~10^{-3} torr), which is similar to the degassing condition of UiO-66 for recycling of adsorbent in CO_2 capture. PXRD patterns were collected after reaching each temperature point. Among the amines that we used to impregnate UiO-66, we chose PENTAEN to study further because of (1) high nitrogen content for high CO_2 capture, (2) high boiling points for viable cycle life, (3) facile diffusion and less steric hindrance than branched amines, and (4) moderate molecular weight (Mw = 232.37) between high molecular weight of PEI and low molecular weight of EN (Mw = 60.1). In-situ temperature resolved PXRD analysis of UiO-66-PENTAEN shows noticeable structural deformation when temperature is gradually raised to 200 °C (Fig. 3). Although PXRD patterns look intact when full pattern is shown, there are slight but important changes. If we focus on two noticeable peaks in the low angle region (2θ = 7–9°), the low angle diffraction patterns indicate a significant shift in the peak positions especially over 150 °C. This peak shift to higher 2 theta was observed in all collected range (2θ = 5–50°). Intensity diminished while increasing temperature up to 200 °C, and was not recovered when temperature returned to room temperature. If amine impregnated UiO-66 is poised for a CO_2

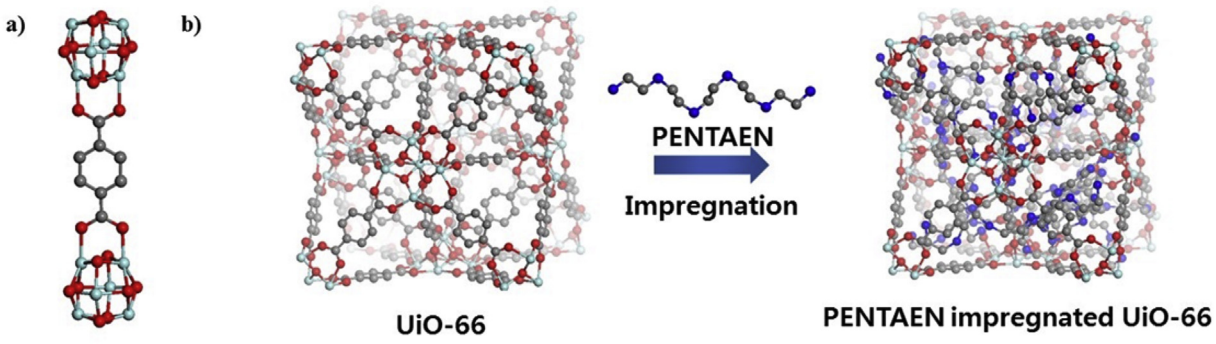

Fig. 1. a) Representative structural information on SBUs and 1,4-benzenedicarboxylate linkers in UiO-66, b) illustrative description of PENTAEN impregnation in UiO-66. Color coding: Carbon (black), nitrogen (blue), oxygen (red), and zirconium (cyan). Hydrogens were removed for clarity. (For interpretation of the references to colour in this figure legend, the reader is referred to the web version of this article.)

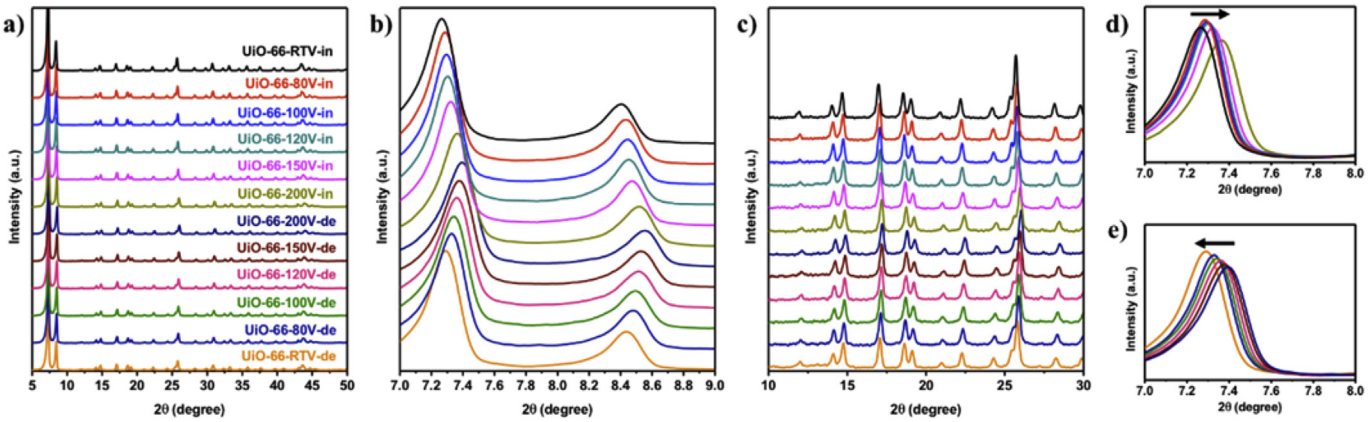

Fig. 2. In-situ temperature resolved PXRD patterns of UiO-66; a) full pattern from 5° to 50°, b) magnified from 7° to 9°, c) magnified from 10° to 30°, d) overlapped patterns with increase in temperature from 7–8°, e) overlapped patterns with decrease in temperature from 7–8°. UiO-66-XV-Z; X, V, and Z refer to temperature, vacuum, and increase or decrease in temperature, respectively.

adsorbent, these observations become critical since analysis conditions mimic regeneration of sorbents in CO_2 capture [48,60,61].

PXRD patterns of UiO-66 and UiO-66-PENTAEN were also compared (Fig. 4). Diffraction at room temperature shows slight shift in UiO-66-PENTAEN. As temperature was increased, both patterns were shifted to higher 2 theta region. However, the gap between two samples was noticeable, meaning UiO-66-PENTAEN accelerated 2 theta shift with reduced intensity (Note that the intensity of UiO-66-PENTAEN was exaggerated by 5 times.). Also, decrease in temperature returned PXRD patterns of UiO-66, whereas PXRD pattern of UiO-66-PENTAEN was not recovered.

To study the effect of chain length of linear amines on PXRD patterns, five different linear amines (EN, DIEN, TRIEN, TETRAEN, PENTAEN) were added to activated UiO-66 (Fig. S3). The PXRD patterns of all the amine impregnated UiO-66 are different from that of UiO-66 except for UiO-66-PENTAEN. Indeed, the resulting PXRD pattern is similar when longer chain was impregnated. UiO-66-250V-EN shows rather clean crystal but PXRD pattern is different from UiO-66-250V, meaning that the crystal structure is not the same as UiO-66. We suspect longer chain of PENTAEN did not affect PXRD pattern. Impregnation of TRIEN and DIEN made dehydrated UiO-66 amorphous, resulting in most of the peaks to be unclear except for broadened low angle diffraction below 10°. Meanwhile, UiO-66-EN shows clear but peculiar PXRD pattern, which is not the same as original UiO-66. The two noticeable peaks at low angle (2θ = ~6.5° and ~8°) do not match with the two major peaks at the similar angle region in the original PXRD pattern of UiO-66. These results contribute to the degree of uncertainty, hence questionable use in reversible CO_2 capture operations.

We assessed how amine loading affects overall performance in porosity and CO_2 capture. Different concentrations of PENTAEN were loaded in activated UiO-66 in order to study the effect of amine loading on specific surface area and CO_2 uptake (Fig. 5 and Table 1). Amine loading was confirmed by elemental analysis in which nitrogen content was increased from 0.14% up to 8.78%. The specific surface area and porosity of bare UiO-66 is in line with other reports [56,62]. Activated UiO-66 shows isotherm of *Type I*, which is attributed to a highly microporous structure [63]. The BET specific surface area of as-synthesized UiO-66 is 1162 m^2/g, with a pore volume of 0.51 cm^3/g (Model: NLDFT, N_2 adsorption on carbon finite pores). Pore size distribution shows two noticeable pore sizes (0.5 nm and 1.2 nm), which are tetrahedral and octahedral pores of UiO-66, respectively [64]. The trace amount of nitrogen in bare UiO-66 is originated from DMF residue coordinated in SBU or trapped in pores. However, all the amine loaded UiO-66 dried at 150 °C under vacuum exhibit almost no accessible surface area with *Type II* isotherms, which can be observed in non-porous or macroporous materials. One possible reason is that the pores of UiO-66 were

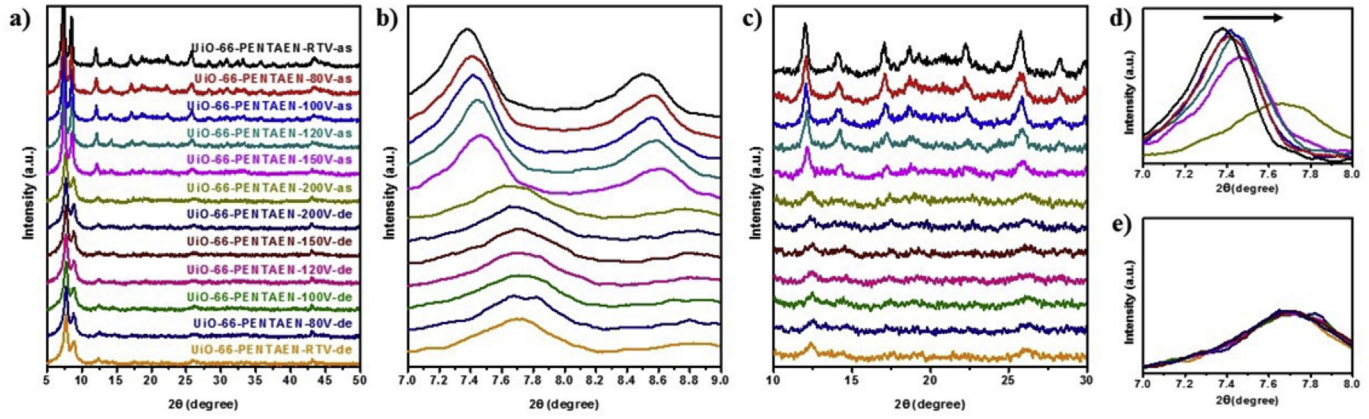

Fig. 3. In-situ temperature resolved PXRD patterns of UiO-66-PENTAEN; a) full pattern from 5° to 50°, b) magnified from 7° to 9°, c) magnified from 10° to 30°, d) overlapped patterns with increase in temperature from 7–8°, e) overlapped patterns with decrease in temperature from 7–8°. UiO-66-PENTAEN-XV-Z; X, V, and Z refer to temperature, vacuum, and increase or decrease in temperature, respectively.

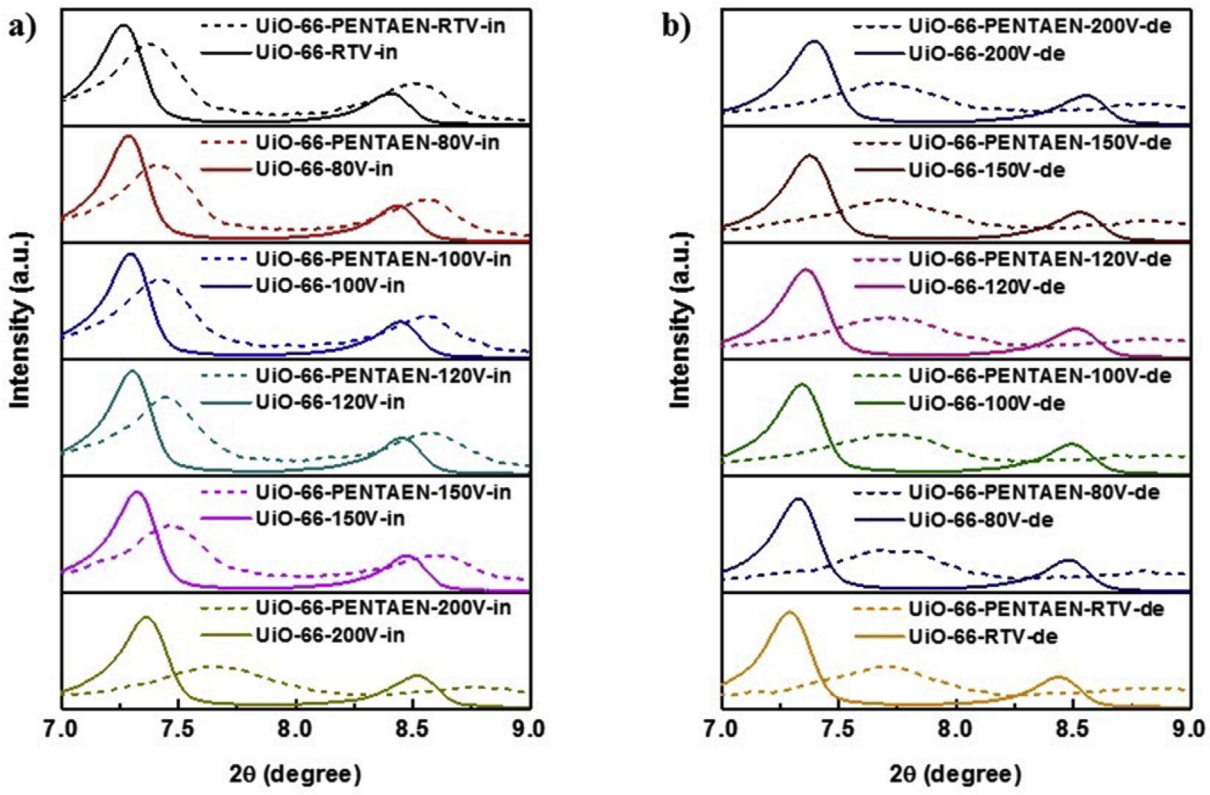

Fig. 4. In-situ temperature resolved PXRD patterns of UiO-66 and UiO-66-PENTAEN by a) overlapped patterns with increase in temperature from 7–9°, b) decrease in temperature from 7–9°. Intensity of UiO-66-PENTAEN was multiplied by five for clarity.

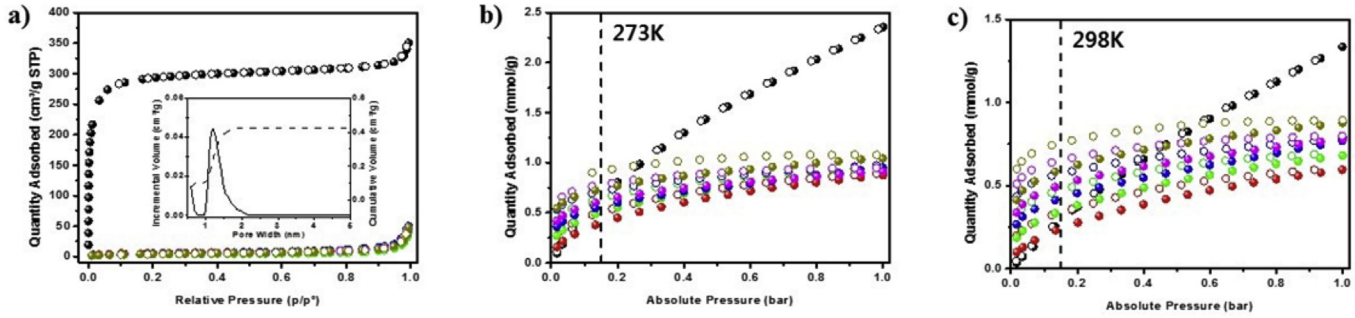

Fig. 5. a) N_2 adsorption (filled) and desorption (open) of UiO-66 and UiO-66-PENTAEN-X at 77 K. Inset shows pore size distribution of bare UiO-66 (model: N_2 adsorption on carbon slit pores by NLDFT). CO_2 adsorption (filled) and desorption (open) of UiO-66 and UiO-66-PENTAEN-X (X = 100, 200, 300, 400, 500) at b) 273 K, and c) 298 K. *Color coding:* UiO-66 (black), UiO-66-PENTAEN-100 (red), UiO-66-PENTAEN-200 (green), UiO-66-PENTAEN-300 (blue), UiO-66-PENTAEN-400 (magenta), UiO-66-PENTAEN-500 (dark yellow). (For interpretation of the references to colour in this figure legend, the reader is referred to the web version of this article.)

completely filled with PENTAEN molecules. The other is that the crystal structure was collapsed. Broadening and intensity reduction in the PXRD patterns were observed as PENTAEN loading was increased gradually (Fig. S3). Peaks above 10° disappeared even with low PENTAEN loading, and the highest loading in this study (UiO-66-PENTAEN-500) results in an almost amorphous structure.

Table 1
The BET specific surface area, pore volume, CO_2 uptake, and nitrogen content of UiO-66 and UiO-66-PENTAEN-X (X = 100, 200, 300, 400, 500). Pore volume was calculated by NLDFT (Model: N_2 adsorption on carbon finite pores). Nitrogen content was obtained by elemental analysis. Qst value is at zero coverage.

	S_{BET} (m^2/g)	Pore volume (cm^3/g)	CO_2 uptake (mmol/g) (298 K, 0.15 bar)	Q_{st} (kJ/mol)	N (%)
UiO-66	1162	0.474	0.29	28.11	0.14
UiO-66-PENTAEN-100	19.97	0.073	0.24	35.03	5.57
UiO-66-PENTAEN-200	14.84	0.064	0.34	37.07	6.87
UiO-66-PENTAEN-300	18.08	0.076	0.42	40.03	7.47
UiO-66-PENTAEN-400	16.54	0.069	0.50	31.46	8.27
UiO-66-PENTAEN-500	16.77	0.073	0.59	45.17	8.78

We suspect high amine loading combined with high temperature under vacuum deteriorates the crystal structure of UiO-66.

The UiO-66-PENTAEN-X shows noticeable enhancement in CO_2 adsorption capacity at 0.15 bar, which is the industrially relevant partial pressure of CO_2 in post-combustion flue gas mixture (Fig. 5 and Table 1) [7,28]. It is clear that CO_2 uptake increased as more PENTAEN was loaded. Hysteresis between CO_2 adsorption and desorption is also evident as PENTAEN loading was increased, which is attributed to enhanced chemisorption. Isosteric heat of adsorption (Qst), which is calculated from CO_2 isotherms at 273 K and 298 K, has a tendency to increase as more PENTAEN was impregnated (Table 1). Qst value of UiO-66-PENTAEN-500 is 45.17 kJ/mol, which is 160% enhanced value of bare UiO-66 (28.11 kJ/mol). Optimized Qst is a crucial need in efficient CO_2 capture because low heat of adsorption leads to low selectivity, and high heat of adsorption leads to high regeneration energy demand [28].

4. Conclusions

In summary, even though UiO-66 is well known for its impeccable mechanical, chemical, and thermal stability, structural deformation was observed when linear amines were impregnated in the structure. From room temperature to 200 °C, PENTAEN impregnated UiO-66 shows irreversible changes in PXRD patterns, whereas pristine UiO-66 shows reversible peak shift. Also, the extent of deformation follows the amine loading amount, which was shown by gradual decrease in the intensity of PXRD patterns. Several linear amines impregnated in activated UiO-66 results in significant peak broadenings in PXRD patterns. Our results show that even zirconium based MOFs, which is known for their outstanding stability, has issues with chemical stability over CO_2 capture sorbent regeneration cycles. Therefore, each new proposed sorbent need to be thoroughly scrutinized by in situ techniques.

Acknowledgement

This work was supported by the National Research Foundation of Korea (NRF) grant funded by the Korea government (MSIP) (No. NRF-2016R1A2B4011027).

Appendix A. Supplementary data

Supplementary data related to this article can be found at http://dx.doi.org/10.1016/j.micromeso.2017.02.021.

References

[1] Q.A. Wang, J.Z. Luo, Z.Y. Zhong, A. Borgna, Energy Environ. Sci. 4 (2011) 42.
[2] A. Samanta, A. Zhao, G.K.H. Shimizu, P. Sarkar, R. Gupta, Ind. Eng. Chem. Res. 51 (2012) 1438.
[3] Y.S. Bae, R.Q. Snurr, Angew. Chem. Int. Ed. 50 (2011) 11586.
[4] S. Choi, J.H. Drese, C.W. Jones, ChemSusChem 2 (2009) 796.
[5] F. Karadas, C.T. Yavuz, S. Zulfiqar, S. Aparicio, G.D. Stucky, M. Atilhan, Langmuir 27 (2011) 10642.
[6] G.T. Rochelle, Science 325 (2009) 1652.
[7] D.M. D'Alessandro, B. Smit, J.R. Long, Angew. Chem. Int. Ed. 49 (2010) 6058.
[8] H.Q. Yang, Z.H. Xu, M.H. Fan, R. Gupta, R.B. Slimane, A.E. Bland, I. Wright, J. Environ. Sci. China 20 (2008) 14.
[9] P. Nugent, Y. Belmabkhout, S.D. Burd, A.J. Cairns, R. Luebke, K. Forrest, T. Pham, S.Q. Ma, B. Space, L. Wojtas, M. Eddaoudi, M.J. Zaworotko, Nature 495 (2013) 80.
[10] R. Dawson, E. Stockel, J.R. Holst, D.J. Adams, A.I. Cooper, Energy Environ. Sci. 4 (2011) 4239.
[11] D. Thirion, V. Rozyyev, J. Park, J. Byun, Y. Jung, M. Atilhan, C.T. Yavuz, Phys. Chem. Chem. Phys. 18 (2016) 14177.
[12] H.A. Patel, D. Ko, C.T. Yavuz, Chem. Mater. 26 (2014) 6729.
[13] T. Islamoglu, T. Kim, Z. Kahveci, O.M. El-Kadri, H.M. El-Kaderi, J. Phys. Chem. C 120 (2016) 2592.
[14] S. Fischer, A. Schimanowitz, R. Dawson, I. Senkovska, S. Kaskel, A. Thomas, J. Mater. Chem. A 2 (2014) 11825.
[15] H. Lee, C.T. Yavuz, Microporous Mesoporous Mater. 229 (2016) 44.
[16] T.M. McDonald, W.R. Lee, J.A. Mason, B.M. Wiers, C.S. Hong, J.R. Long, J. Am. Chem. Soc. 134 (2012) 7056.
[17] V. Zelenak, M. Badanicova, D. Halamova, J. Cejka, A. Zukal, N. Murafa, G. Goerigk, Chem. Eng. J. 144 (2008) 336.
[18] M.G. Plaza, C. Pevida, A. Arenillas, F. Rubiera, J.J. Pis, Fuel 86 (2007) 2204.
[19] H.A. Patel, S.H. Je, J. Park, D.P. Chen, Y. Jung, C.T. Yavuz, A. Coskun, Nat. Commun. 4 (2013) 1357.
[20] R. Sanz, G. Calleja, A. Arencibia, E.S. Sanz-Perez, Appl. Surf. Sci. 256 (2010) 5323.
[21] S.B. Yang, L. Zhan, X.Y. Xu, Y.L. Wang, L.C. Ling, X.L. Feng, Adv. Mater. 25 (2013) 2130.
[22] Y.C. Lin, Q.J. Yan, C.L. Kong, L. Chen, Sci. Rep. 3 (2013) 1859.
[23] A.R. Millward, O.M. Yaghi, J. Am. Chem. Soc. 127 (2005) 17998.
[24] R.E. Morris, P.S. Wheatley, Angew. Chem. Int. Ed. 47 (2008) 4966.
[25] G. Ferey, C. Serre, T. Devic, G. Maurin, H. Jobic, P.L. Llewellyn, G. De Weireld, A. Vimont, M. Daturi, J.S. Chang, Chem. Soc. Rev. 40 (2011) 550.
[26] S. Kitagawa, R. Kitaura, S. Noro, Angew. Chem. Int. Ed. 43 (2004) 2334.
[27] J.R. Li, R.J. Kuppler, H.C. Zhou, Chem. Soc. Rev. 38 (2009) 1477.
[28] K. Sumida, D.L. Rogow, J.A. Mason, T.M. McDonald, E.D. Bloch, Z.R. Herm, T.H. Bae, J.R. Long, Chem. Rev. 112 (2012) 724.
[29] C.L. Hobday, R.J. Marshall, C.F. Murphie, J. Sotelo, T. Richards, D.R. Allan, T. Duren, F.X. Coudert, R.S. Forgan, C.A. Morrison, S.A. Moggach, T.D. Bennett, Angew. Chem. Int. Ed. 55 (2016) 2401.
[30] S. Keskin, T.M. van Heest, D.S. Sholl, Chemsuschem 3 (2010) 879.
[31] D. Alezi, Y. Belmabkhout, M. Suyetin, P.M. Bhatt, L.J. Weselinski, V. Solovyeva, K. Adil, I. Spanopoulos, P.N. Trikalitis, A.H. Emwas, M. Eddaoudi, J. Am. Chem. Soc. 137 (2015) 13308.
[32] A. Santra, M.S. Lah, P.K. Bharadwaj, Z. Anorg. Allg. Chem. 640 (2014) 1134.
[33] X. Song, M. Oh, M.S. Lah, Inorg. Chem. 52 (2013) 10869.
[34] O.M. Yaghi, M. O'Keeffe, N.W. Ockwig, H.K. Chae, M. Eddaoudi, J. Kim, Nature 423 (2003) 705.
[35] I. Erucar, S. Keskin, Ind. Eng. Chem. Res. 55 (2016) 1929.
[36] M. Kim, S.J. Garibay, S.M. Cohen, Inorg. Chem. 50 (2011) 729.
[37] Z.Q. Wang, S.M. Cohen, Chem. Soc. Rev. 38 (2009) 1315.
[38] H. Furukawa, K.E. Cordova, M. O'Keeffe, O.M. Yaghi, Science 341 (2013) 974.
[39] H. Wu, W. Zhou, T. Yildirim, J. Am. Chem. Soc. 131 (2009) 4995.
[40] A.O. Yazaydin, A.I. Benin, S.A. Faheem, P. Jakubczak, J.J. Low, R.R. Willis, R.Q. Snurr, Chem. Mater. 21 (2009) 1425.
[41] E.D. Bloch, W.L. Queen, R. Krishna, J.M. Zadrozny, C.M. Brown, J.R. Long, Science 335 (2012) 1606.
[42] Y.Y. Liu, R.C. Klet, J.T. Hupp, O. Farha, Chem. Commun. 52 (2016) 7806.
[43] A.E. Platero-Prats, A. Mavrandonakis, L.C. Gallington, Y.Y. Liu, J.T. Hupp, O.K. Farha, C.J. Cramer, K.W. Chapmant, J. Am. Chem. Soc. 138 (2016) 4178.
[44] D. Yang, S.O. Odoh, J. Borycz, T.C. Wang, O.K. Farha, J.T. Hupp, C.J. Cramer, L. Gagliardi, B.C. Gates, ACS Catal. 6 (2016) 235.
[45] N.C. Burtch, H. Jasuja, K.S. Walton, Chem. Rev. 114 (2014) 10575.
[46] J.B. Decoste, G.W. Peterson, M.W. Smith, C.A. Stone, C.R. Willis, J. Am. Chem. Soc. 134 (2012) 1486.
[47] J.H. Cavka, S. Jakobsen, U. Olsbye, N. Guillou, C. Lamberti, S. Bordiga, K.P. Lillerud, J. Am. Chem. Soc. 130 (2008) 13850.
[48] L. Valenzano, B. Civalleri, S. Chavan, S. Bordiga, M.H. Nilsen, S. Jakobsen, K.P. Lillerud, C. Lamberti, Chem. Mater. 23 (2011) 1700.
[49] M. Kandiah, M.H. Nilsen, S. Usseglio, S. Jakobsen, U. Olsbye, M. Tilset, C. Larabi, E.A. Quadrelli, F. Bonino, K.P. Lillerud, Chem. Mater. 22 (2010) 6632.
[50] M. Kandiah, S. Usseglio, S. Svelle, U. Olsbye, K.P. Lillerud, M. Tilset, J. Mater. Chem. 20 (2010) 9848.
[51] M.J. Cliffe, W. Wan, X.D. Zou, P.A. Chater, A.K. Kleppe, M.G. Tucker, H. Wilhelm, N.P. Funnell, F.X. Coudert, A.L. Goodwin, Nat. Commun. 5 (2014) 4176.
[52] J.E. Mondloch, M.J. Katz, N. Planas, D. Semrouni, L. Gagliardi, J.T. Hupp, O.K. Farha, Chem. Commun. 50 (2014) 8944.
[53] L.J. Li, P.Q. Liao, C.T. He, Y.S. Wei, H.L. Zhou, J.M. Lin, X.Y. Li, J.P. Zhang, J. Mater. Chem. A 3 (2015) 21849.
[54] S.K. Xian, Y. Wu, J.L. Wu, X. Wang, J. Xiao, Ind. Eng. Chem. Res. 54 (2015) 11151.
[55] J.A. Mason, K. Sumida, Z.R. Herm, R. Krishna, J.R. Long, Energy Environ. Sci. 4 (2011) 3030.
[56] M.J. Katz, Z.J. Brown, Y.J. Colon, P.W. Siu, K.A. Scheidt, R.Q. Snurr, J.T. Hupp, O.K. Farha, Chem. Commun. 49 (2013) 9449.
[57] G.C. Shearer, S. Chavan, J. Ethiraj, J.G. Vitillo, S. Svelle, U. Olsbye, C. Lamberti, S. Bordiga, K.P. Lillerud, Chem. Mater. 26 (2014) 4068.
[58] D. Dubbeldam, K.S. Walton, D.E. Ellis, R.Q. Snurr, Angew. Chem. Int. Ed. 46 (2007) 4496.
[59] S. Jakobsen, D. Gianolio, D.S. Wragg, M.H. Nilsen, H. Emerich, S. Bordiga, C. Lamberti, U. Olsbye, M. Tilset, K.P. Lillerud, Phys. Rev. B 86 (2012).
[60] J.B. DeCoste, G.W. Peterson, H. Jasuja, T.G. Glover, Y.G. Huang, K.S. Walton, J. Mater. Chem. A 1 (2013) 5642.
[61] C.G. Piscopo, A. Polyzoidis, M. Schwarzer, S. Loebbecke, Microporous Mesoporous Mater. 208 (2015) 30.
[62] G.E. Cmarik, M. Kim, S.M. Cohen, K.S. Walton, Langmuir 28 (2012) 15606.
[63] K.S.W. Sing, D.H. Everett, R.A.W. Haul, L. Moscou, R.A. Pierotti, J. Rouquerol, T. Siemieniewska, Pure Appl. Chem. 57 (1985) 603.
[64] M. Kim, S.M. Cohen, CrystEngComm 14 (2012) 4096.